

Article

Oxidase-like MOF-818 Nanozyme with High Specificity for Catalysis of Catechol Oxidation

Minghua Li, Jinxing Chen, Weiwei Wu, Youxing Fang, and Shaojun Dong

J. Am. Chem. Soc., **Just Accepted Manuscript** • DOI: 10.1021/jacs.0c07273 • Publication Date (Web): 13 Aug 2020

Downloaded from pubs.acs.org on August 13, 2020

Just Accepted

“Just Accepted” manuscripts have been peer-reviewed and accepted for publication. They are posted online prior to technical editing, formatting for publication and author proofing. The American Chemical Society provides “Just Accepted” as a service to the research community to expedite the dissemination of scientific material as soon as possible after acceptance. “Just Accepted” manuscripts appear in full in PDF format accompanied by an HTML abstract. “Just Accepted” manuscripts have been fully peer reviewed, but should not be considered the official version of record. They are citable by the Digital Object Identifier (DOI®). “Just Accepted” is an optional service offered to authors. Therefore, the “Just Accepted” Web site may not include all articles that will be published in the journal. After a manuscript is technically edited and formatted, it will be removed from the “Just Accepted” Web site and published as an ASAP article. Note that technical editing may introduce minor changes to the manuscript text and/or graphics which could affect content, and all legal disclaimers and ethical guidelines that apply to the journal pertain. ACS cannot be held responsible for errors or consequences arising from the use of information contained in these “Just Accepted” manuscripts.

Oxidase-like MOF-818 Nanozyme with High Specificity for Catalysis of Catechol Oxidation

Minghua Li, § [a,b] Jinxing Chen, § [b,c] Weiwei Wu, [b,c] Youxing Fang, * [b] Shaojun Dong* [a,b,c]

[a] College of Chemistry, Jilin University, Changchun, 130012, P.R. China.

[b] State Key Laboratory of Electroanalytical Chemistry, Changchun Institute of Applied Chemistry, Chinese Academy of Sciences, Changchun, 130022, P. R. China.

[c] University of Science and Technology of China, Hefei, Anhui, 230026, P.R. China.

ABSTRACT: Despite the extensive studies of the nanozymes showing their superior properties compared to natural enzymes and traditional artificial enzymes, the development of highly specific nanozymes is still a challenge. The catechol oxidase specifically catalyzing the oxidations of *o*-diphenol to the corresponding *o*-quinone is important to the biosynthesis of melanin and other polyphenolic natural products. In this study, we firstly propose that MOF-818, containing trinuclear copper centers mimicking the active sites of natural catechol oxidase, shows the efficient catechol oxidase activity with good specificity and no peroxidase-like characteristics. MOF-818 has good specificity and high catalytic activity as a novel catechol oxidase nanozyme.

INTRODUCTION

Nanomaterials with enzymatic activities (nanozyme) have been comprehensively investigated due to their high stability, high catalytic efficiency, low price and conveniences of preparation.¹⁻³ Nanozymes are considered to be excellent substitutes for natural enzymes.⁴⁻⁶ So far, a large number of nanomaterials with enzyme-like activity have been discovered and designed, including metals,⁷⁻⁸ metal oxides,⁹⁻¹¹ metal-organic frameworks (MOFs)¹²⁻¹⁶ and carbon-based materials.¹⁷⁻¹⁸ According to the types of catalysis, nanozymes can be classified into oxidase mimic,¹⁹ peroxidase mimic,²⁰⁻²¹ superoxide dismutase mimic,²²⁻²³ catalase mimic²⁴ and hydrolase mimic,²⁵⁻²⁶ etc. Due to the excellent performances of nanozymes, various nanozymes have been extensively studied for the applications of biosensors,²⁷⁻²⁸ environmental protections,²⁹ disease diagnosis and treatments,³⁰ and antibacterial agents.³¹

Despite the increasing interests in nanozymes, the development of highly specific nanozymes is still a challenge. Oxidase nanozyme has been widely studied as an important topic of nanozymes, while the previously reported metal oxides and noble metals based nanozymes applied to oxidase mimics still show peroxidase-like activity, which merely use 3,3',5,5'-tetramethylbenzidine (TMB) and 2,2'-azino-bis(3-ethylbenzothiazoline-6-sulfonic acid (ABTS) as universal substrates. TMB and ABTS are typical substrates of peroxidase to certify the peroxidase activity, and not qualified to characterize oxidase activity. Currently, oxidase nanozymes have a similar mechanism by activating molecular O₂ to yield reactive oxygen species, which subsequently oxidize the substrates and process the whole reactions. Accordingly, the reported oxidase nanozymes usually exhibit low specificities because they can catalyze the oxidation of a variety of reducing substrates including ABTS, TMB, *o*-phenylenediamine (OPD), ascorbic acid, ethanol, catechol, and glutathione.³²⁻³⁶ Designing nanozymes by simulating the structural characteristics of natural enzymes is a feasible strategy to improve the specificities of nanozymes.

Polyphenol oxidases include tyrosinase and catechol oxidase. In vivo, tyrosinase plays an important role in the biosynthesis of melanin and other polyphenolic natural products,³⁷ while catechol oxidase catalyzes the oxidation of substrates into corresponding *o*-quinones which can be polymerized to produce melanin and form an insoluble barrier to protect the damaged plant from pathogens or insects.³⁸ Since polyphenol oxidases have significant biological effects, it is necessary to explore nanomaterials to mimic polyphenol oxidases and their related catalytic mechanisms.

In this work, we demonstrate that a MOF based nanomaterial, MOF-818, catalyzes the oxidation of catechols, but shows no peroxidase-like activity. Moreover, by mimicking the active center of natural catechol oxidase, MOF-818 exhibits higher catalytic ability and specificity than the reported oxidation nanozymes. 3,5-di-*tert*-butylcatechol (3,5-DTBC) was selected as the substrate for studying catechol oxidase activity because it has superior solubility and is infeasible to be polymerized than other catechol derivatives. MOF-818 exhibits the catalytic behaviors similar to natural catechol oxidase, which is completely different from the previously reported oxidase nanozymes. Natural catechol oxidases, containing a coupled binuclear copper metal center coordinated by six histidines as the active site, catalyzes the oxidation of *o*-diphenol, while O₂ is reduced to peroxide in the ternary enzyme-catechol-dioxygen complex, and then protonated to form water by the cleavage of the O-O bond.³⁹ Similarly, MOF-818 catalyzes the oxidation of *o*-diphenols by trinuclear copper centers in the presence of O₂ and generates H₂O₂ rather than H₂O. Therefore, MOF-818 has good specificity and high catalytic activity as a novel catechol oxidase nanozyme.

RESULTS AND DISCUSSION

MOF-818 was prepared by the reported method with some modifications.⁴⁰ MOF-818 is with trinuclear copper centers, and TEM and SEM images revealed that most of the as-

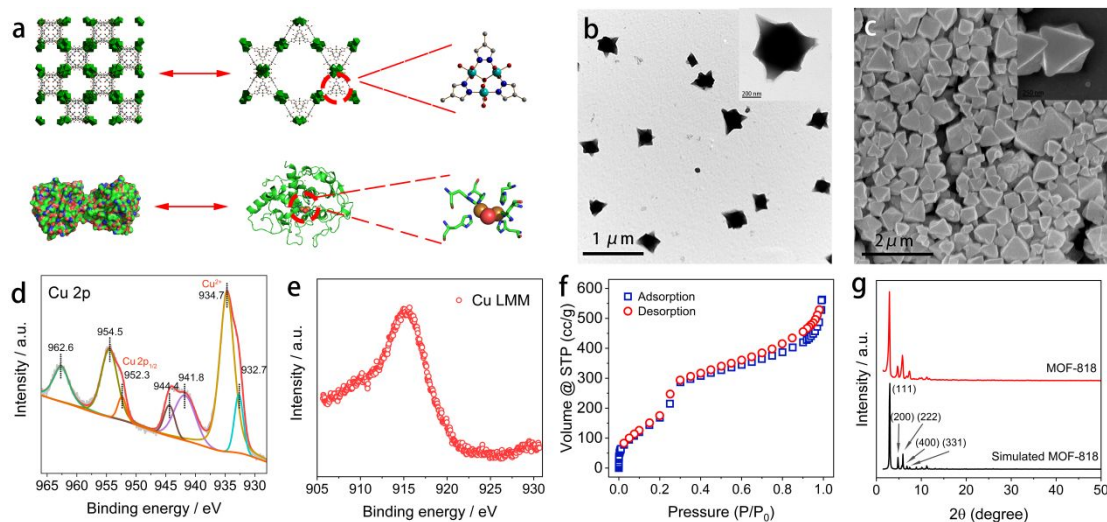


Figure 1. (a) Structure of MOF-818 and catechol oxidase (PDB: 1BT1). Color code: blue (N), white (C), red (O), turquoise (Cu). (b) TEM images of MOF-818. (c) SEM images of MOF-818. (d) Cu 2p XPS spectrum of MOF-818. (e) Cu LMM Auger spectrum of MOF-818. (f) Adsorption-desorption isotherm of nitrogen for MOF-818 at 77 K. (g) Experimental and simulated XRD patterns of MOF-818.

synthesized MOF-818 were octahedron in shape (Figure 1a-c). The elemental composition and chemical bonding were analyzed by X-ray photoelectron spectroscopy (XPS) (Figure S1). The survey spectra of MOF-818 confirmed the presence of C, O, N, Zr, and Cu, with atomic ratios of 74.66%, 23.47%, 1.32%, 0.23%, and 0.32%, respectively. Inductively coupled plasma atomic emission spectroscopy (ICP-AES) was used to identify the loadings of Cu (10.5 wt %) and Zr (11.9 wt %) (Table S1). The binding energy (BE) of Zr in MOF-818 was 182.5 eV, corresponding to the standard BE of Zr^{4+} (Figure S2). Cu 2p spectrum is shown in Figure 1d. The higher BE peak at 934.7 eV was assigned to Cu^{2+} , accompanied by the characteristic Cu^{2+} shakeup satellite peaks (962.6 eV, 941.8 eV). The lower BE peak at 932.7 eV suggested the presence of Cu^+ and/or Cu^0 species. Because Cu $2p_{3/2}$ XPS cannot differentiate between Cu^+ and Cu^0 , Auger Cu LMM spectrum was collected to confirm the presence of Cu^+ at ~915 eV (Figure 1e). No peak was detected at 918-920 eV, indicating that Cu^0 was absent in MOF-818. Thus MOF-818 contained Cu in the states of Cu^+ and Cu^{2+} . In Figure 1f, N_2 adsorption-desorption isotherm of MOF-818 belonged to type IV isotherm, as it was the typical mesoporous materials. The multipoint BET surface area of MOF-818 was calculated to be 743.5 m^2/g . Pore size distributions for MOF-818 was analyzed as shown in Figure S3. The crystal structure of MOF-818 was characterized by XRD (Figure 1g). MOF-818 possessed an *F*-centered cubic crystal lattice and matched well with the simulated XRD pattern.⁴⁰

The oxidation process was monitored to study the catechol oxidase-like activity of MOF-818 by using UV-vis spectroscopy. As shown in Figure 2a, 3,5-DTBC had a strong absorption at 278 nm and a new absorption peak appeared at 415 nm when it was oxidized to 3,5-di-*tert*-butyl-*o*-benzoquinone (3,5-DTBQ). In the presence of MOF-818, the absorption peak at 415 nm increased significantly over time (Figure 2b). The absorption peak also increased with the increasing concentration of MOF-818 and 3,5-DTBC, indicating the evident enhancement of the reaction rate (Figure 2c-d). Similar phenomena were observed when L-dopa and dopamine were used as the substrates (Figure S4), demonstrating that MOF-818 possessed catechol oxidase-like

activity. MOF-818 is stable in aqueous solution with various pH values.⁴⁰ The catechol oxidase-like activities of MOF-818 at different values of pH and temperature were measured. The catalytic activity of MOF-818 gradually increased with increasing pH value and temperature, and the rising trend slowed down above pH 8 (Figure 2e-f). Therefore, PBS (pH 8.0) was used for further assays.

MOF-808, containing Zr ions only, was synthesized and studied as the control. The TEM images revealed that most of the as-synthesized MOF-808 samples were octahedrons in shape and similar to that of MOF-818 (Figure S5). The crystal structure of MOF-808 was characterized by XRD, which matched well with the simulated XRD patterns (Figure S6). As shown in Figure 3a, MOF-808 only had weak catechol oxidase activity in contrast to MOF-818, indicating that Cu but not Zr constructed the active center of MOF-818. Compared to the absorption at 415 nm in the air-saturated buffer, the absorption

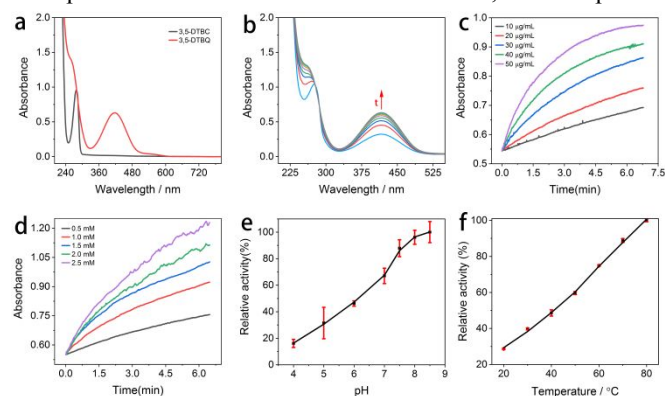


Figure 2. (a) UV-vis absorption spectra of 3,5-DTBC and 3,5-DTBQ. (b) UV-vis absorption spectra over time in the presence of 0.5 mM 3,5-DTBC and 50 $\mu g/mL$ MOF-818. (c, d) Time-dependent absorbance at 415 nm with different concentrations of MOF-818 in the presence of 0.5 mM 3,5-DTBC (c) and different concentrations of 3,5-DTBC in the presence of 50 $\mu g/mL$ MOF-818 (d). Catechol oxidase-like activities of MOF-818 at different pH values (e) and temperatures (f).

of 3,5-DTBC catalyzed by MOF-818 showed a significant increase in O₂-saturated condition and a decrease in N₂-saturated condition. These suggested that oxygen was necessary for this reaction (Figure 3b). To verify the production during the reaction catalyzed by MOF-818, horseradish peroxidase (HRP) and TMB were added to the solution of MOF-818 and 3,5-DTBC (Figure 3c). When HRP and TMB were both added to a mixed solution of MOF-818 and 3,5-DTBC, the characteristic absorption peak of oxidized TMB appeared at 650 nm, indicating that H₂O₂ was generated in the reaction. At the same time, due to the presence of oxidized TMB, the absorption peak at 415 nm increased significantly (Figure S7). However, when HRP and TMB were added to a solution with either MOF-818 or 3,5-DTBC, the absorption at 650 nm cannot be detected at all (Figure 3d). The presence of H₂O₂ was further confirmed by Electron Paramagnetic Resonance (EPR) in Figure 3e. Additionally, EPR spectrum of Figure 3f proved the formation of *o*-semiquinone radical in the system. Therefore, in this cascade reaction, 3,5-DTBC is oxidized by O₂ accompanied by the formation of H₂O₂, which further oxidizes TMB with the catalysis of HRP. Further experimental results showed that regardless of the presence of catalyst MOF-818 or not, H₂O₂ had no substantial catalytic effect on the oxidation of 3,5-DTBC (Figure S8), indicating that the effect of H₂O₂ on the catechol oxidase-like activity of MOF-818 is negligible under the reaction conditions.

The catalytic effects of MOF-818 on different kinds of substrates including TMB and ABTS were studied. Under alkaline condition, the catalyst showed excellent catalytic activity for 3,5-DTBC, but was unable to catalyze the oxidation of TMB and ABTS (Figure S9). Under acidic condition, MOF-818 can also slowly promote the oxidation of 3,5-DTBC (Figure S10) without the ability to catalyze the oxidation of TMB (Figure 4a). Moreover, CeO₂ and Pt NPs were synthesized to compare with MOF-818 in the catalysis (Figure S5). MOF-818 specifically catalyzed the oxidation of 3,5-DTBC without obvious peroxidase-like activity, while CeO₂ and Pt NPs can catalyze the oxidation of TMB and 3,5-DTBC and exhibit both oxidase-like and peroxidase-like activities (Figure 4a-d). Since the natural catechol oxidases do not possess peroxidase activity, MOF-818 is the best candidate as the nanozyme to mimic catechol oxidase among the varieties of oxidase nanozyme. MOF-818 also showed higher catalytic ability than that of previously reported catechol nanozymes such as CeO₂ and Pt NPs (Figure. 4c). Based on the above results, MOF-818 with good specificity and high catalytic activity had been certificated as a new catechol oxidase nanozyme.

The possible reaction mechanism is proposed as illustrated in Figure S11. 3,5-DTBC is oxidized to 3,5-DTBQ by tricopper(II) centers to form the copper(I) species in a fast reaction step. It is demonstrated that Cu(II) has the ability to oxidize a large number of organic compounds.³⁷ O₂ is necessary for the catalytic reaction and plays the role to reoxidize copper(I) generated during the catalytic cycle while H₂O₂ is produced in a slow, rate-determining step. This conjecture is well proved by the effect of oxygen concentration on the reaction. The absorption peak at 415 nm increased significantly in O₂-saturated condition compared to the absorption in the air-saturated buffer, indicating that oxygen engages the reaction as the oxidant. Although there was a slight decrease in N₂-saturated buffer, the absorption

peak still showed a strong signal that can be attributed to the oxidation by Cu(II) (Figure 3b). On the other hand, the reported oxidase nanozymes catalyze the oxidation by activating O₂ to yield reactive oxygen species, which indistinguishably oxidize the substrates. Thus, they can catalyze the oxidation of a variety of reducing substrates. Oppositely, MOF-818 selectively catalyzes the oxidation of 3,5-DTBC but not TMB and ABTS, proving that the reaction mechanism is completely different from the conventional oxidase nanozyme reported.

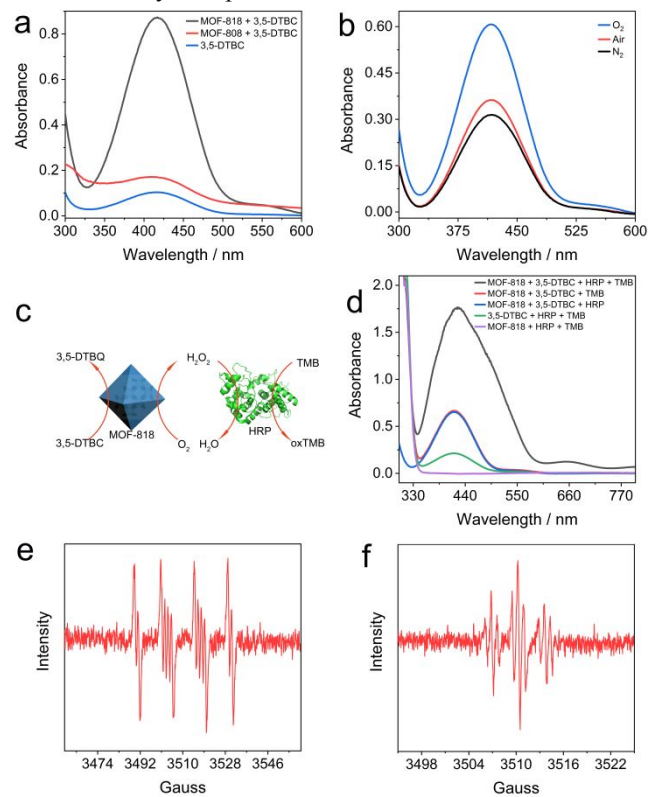


Figure 3. (a) UV-vis absorption spectra of 3,5-DTBC in the absence and presence of 50 µg/mL MOF-818 or MOF-808. The concentration of 3,5-DTBC was 0.5 mM. (b) The UV-vis absorption spectra of 3,5-DTBC in air-saturated, O₂-saturated, and N₂-saturated PBS solution (10 mM pH 8.0) with MOF-818. (c) The scheme of detecting H₂O₂. (d) UV-vis absorption spectra of solutions with several combinations of MOF-818, 3,5-DTBC, HRP and TMB (e) EPR spectrum of H₂O₂ in the reaction system. (f) EPR spectrum of *o*-semiquinone radical in the reaction system.

The oxidation rate of 3,5-DTBC was dependent on the concentrations of both MOF-818 and the substrate. Increasing the concentration of either MOF-818 or 3,5-DTBC resulted in an evident enhancement of the reaction rate. The kinetic studies of the oxidation of 3,5-DTBC were carried out by monitoring the concentration of 3,5-DTBQ at 415 nm by varying the concentration of 3,5-DTBC while keeping the MOF-818 concentration constant. The reaction rate was found to follow Michaelis–Menten kinetics. The Lineweaver–Burk plot was calculated from the Michaelis–Menten curve (Figure 5a-b). The enzyme kinetic constants K_m (Michaelis constant) and K_{cat} (catalytic constant) were obtained to measure the enzyme efficiency. The calculated values for V_m , K_m , K_{cat} and

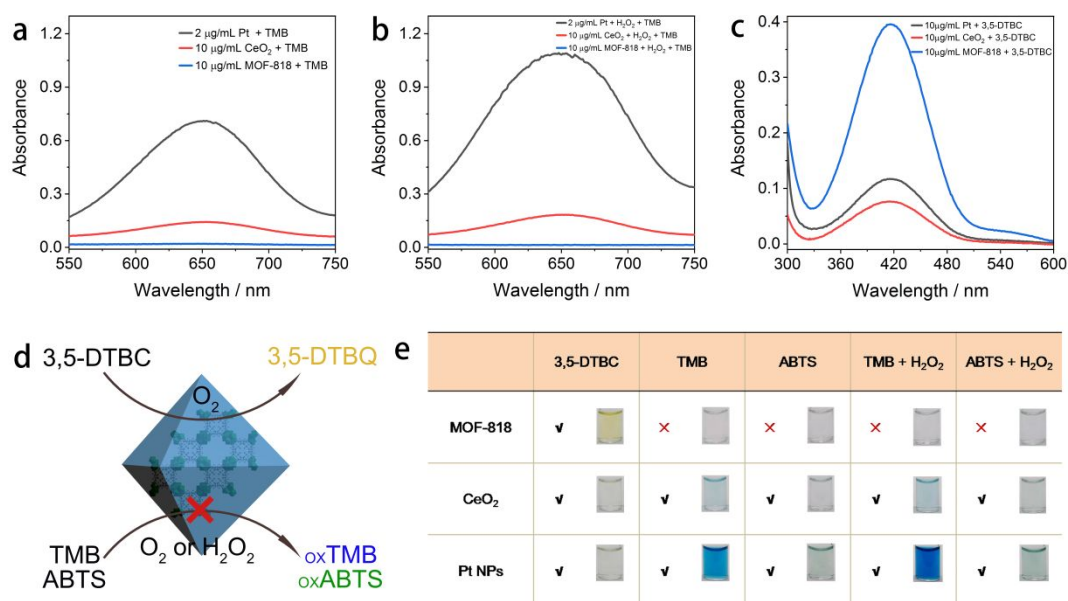


Figure 4. (a, b) UV-vis absorption spectra of the resultant solutions containing TMB and different catalysts in the absence (a) and presence (b) of H₂O₂ in sodium acetate–acetic acid buffer solution (100 mM pH 4.0). (c) UV-vis absorption spectra of 3,5-DTBC in the presence of different catalysts in phosphate buffer (10 mM pH 8.0). (d) Schematic illustration of the activity of MOF-818. (e) The nanozyme activities of MOF-818, CeO₂, and Pt NPs. Insets: the color of solutions with the different substrates and nanozymes.

K_{cat}/K_m were $3.17 \times 10^{-6} \text{ M s}^{-1}$, $8.10 \times 10^{-4} \text{ M}$, 0.383 s^{-1} and $4.73 \times 10^2 \text{ M}^{-1} \text{ s}^{-1}$, respectively, indicating that MOF-818 has excellent catalytic activity as a catechol oxidase mimic. As shown in Figure S12 and Table S2, the enzyme kinetic constants K_m and V_m of CeO₂ and Pt NPs were acquired by using 3,5-DTBC as the substrate under the same conditions. The results show that MOF-818 exhibits much higher catalytic efficiency than CeO₂ and Pt NPs.

To determine the product and calculate the yield, the UV-vis spectra of a standard sample of 3,5-DTBQ and 3,5-DTBC catalyzed by MOF-818 were collected (Figure S13a). The results confirmed that the product of the oxidation was 3,5-DTBQ. The standard curve of 3,5-DTBQ was measured (Figure S13b). According to the absorbance plateau reached (Figure S13c-d), 0.5 mM of 3,5-DTBC catalyzed by 30 $\mu\text{g}/\text{mL}$ of MOF-818 granted the yield of 98.2%.

The stability of MOF-818 has been tested by recycling experiments and the reusable MOF-818 was characterized by XRD. After four cycles in the HEPES buffer solution (10 mM pH 8.0), MOF-818 still retained 70% of its activity. After five cycles, there was no change in XRD data, indicating that MOF-818 possesses excellent stability (Figure S14).

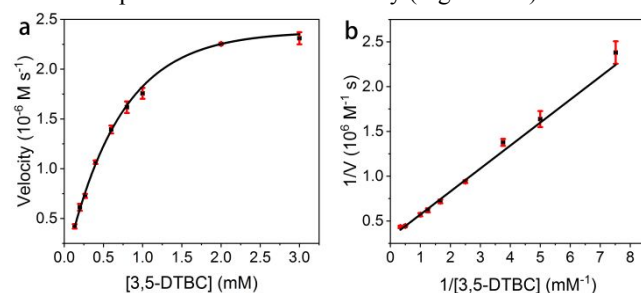


Figure 5. (a) Michaelis–Menten curves for 3,5-DTBC. (b) Lineweaver–Burk plot for determination of kinetic constant of MOF-818 for 3,5-DTBC. The concentration of MOF-818 was 50 $\mu\text{g}/\text{mL}$.

To prove the universality of the catalyst, L-dopa and dopamine were also selected as substrates to examine the activity of the nanozyme. The catalyst showed significant catalytic activities on both substrates. We measured the kinetic constants of L-dopa. The Michaelis–Menten curve and Lineweaver–Burk plot were obtained (Figure S15). The calculated values for V_m , K_m , K_{cat} and K_{cat}/K_m were $7.97 \times 10^{-8} \text{ M s}^{-1}$, $4.8 \times 10^{-4} \text{ M}$, $9.64 \times 10^{-3} \text{ s}^{-1}$, and $20.1 \text{ M}^{-1} \text{ s}^{-1}$, respectively. Compared to 3,5-DTBC, L-dopa lead to a dramatically decreased activity of MOF-818. It is assumed that L-dopa is a relative stable chemical, and the complexation of the amino group in L-dopa and copper in MOF-818 inhibits the activity of the catalyst. As dopamine was used as the substrate, MOF-818 could catalyze the oxidation of dopamine to form polydopamine (Figure S4). Some other catechol derivatives including quercetin, epicatechin and caffeic acid were also oxidized with MOF-818 (Figure S16). Therefore, MOF-818 is the catalyst for the oxidation of *o*-diphenols. Table S2 compared the catalytic abilities of reported catechol oxidase-like nanozymes and natural catechol oxidase.

Phenolic compounds, such as chlorophenol, widely apply for fungicides and preservatives and are common toxic pollutants.⁴¹ These phenolic compounds pose a threat to human health and are widely detected in soil and water, which requires green catalysts for their degradations and detections. It has been reported that potato polyphenol oxidase extracted from commercial potatoes showed excellent catalytic activity for the degradation of pentachlorophenol in the presence of oxygen at room temperature.⁴² So the construction of a nanozyme that mimics the natural enzyme to degrade and detect chlorophenol is a promising strategy. To test the activity of MOF-818, we used 2,4-dichlorophenol (2,4-DP) as the substrate. The oxidation product of 2,4-DP reacted with 4-aminoantipyrine (4-AAP) and generated a red product with an absorbance at 510 nm, as shown in Figure S17. Thus, MOF-818 has excellent catalytic activity as a nanozyme and shows

good prospects in the detection and degradation of chlorophenol.

CONCLUSIONS

In summary, we firstly proposed that MOF-818 has efficient catechol oxidase-like activity with good specificity. MOF-818 can catalyze the oxidation of catechol to the corresponding *o*-quinones but shows no peroxidase activity. The influence of reaction conditions on the catalyst was systematically investigated. Different from the previously reported catechol oxidase nanozymes, MOF-818 catalyzed the oxidation of *o*-diphenols and produced H₂O₂. In the present work, O₂ was necessary and played the role to convert Cu(I) into Cu(II) during the recycling. Moreover, by mimicking the active center of natural catechol oxidase, MOF-818 exhibited specificity and higher catalytic ability than that of the catechol oxidase nanozymes previously reported.

ASSOCIATED CONTENT

The Supporting Information is available free of charge. Experimental details, Figures S1–S17, Tables S1–S2, and additional references.

AUTHOR INFORMATION

Corresponding Author

*dongsj@ciac.ac.cn, *fangxy@ciac.ac.cn.

Author Contributions

§Minghua Li and §Jinxing Chen contributed equally.

Notes

The authors declare no competing financial interest.

ACKNOWLEDGMENT

This work is supported by the National Natural Science Foundation of China (No. 21675151, 21705145 and 21721003) and the Ministry of Science and Technology of China (No. 2016YFA0203203).

REFERENCES

- (1) Gao, L.; Zhuang, J.; Nie, L.; Zhang, J.; Zhang, Y.; Gu, N.; Wang, T.; Feng, J.; Yang, D.; Perrett, S.; Yan, X., Intrinsic peroxidase-like activity of ferromagnetic nanoparticles. *Nat. Nanotech.* **2007**, *2*, 577-83.
- (2) Kotov, N. A., Inorganic Nanoparticles as Protein Mimics. *Science* **2010**, *330*, 188-189.
- (3) Wei, H.; Wang, E., Nanomaterials with enzyme-like characteristics (nanozymes): next-generation artificial enzymes. *Chem. Soc. Rev.* **2013**, *42*, 6060-93.
- (4) Wu, J.; Wang, X.; Wang, Q.; Lou, Z.; Li, S.; Zhu, Y.; Qin, L.; Wei, H., Nanomaterials with enzyme-like characteristics (nanozymes): next-generation artificial enzymes (II). *Chem. Soc. Rev.* **2019**, *48*, 1004-1076.
- (5) Huang, Y.; Ren, J.; Qu, X., Nanozymes: Classification, Catalytic Mechanisms, Activity Regulation, and Applications. *Chem. Rev.* **2019**, *119*, 4357-4412.
- (6) Yuan, Y.; Yang, Y.; Faheem, M.; Zou, X.; Ma, X.; Wang, Z.; Meng, Q.; Wang, L.; Zhao, S.; Zhu, G., Molecularly Imprinted Porous Aromatic Frameworks Serving as Porous Artificial Enzymes. *Adv. Mater.* **2018**, *30*, e1800069.
- (7) Comotti, M.; Della Pina, C.; Falletta, E.; Rossi, M., Aerobic Oxidation of Glucose with Gold Catalyst: Hydrogen Peroxide as Intermediate and Reagent. *Adv. Synth. Catal.* **2006**, *348*, 313-316.
- (8) Yu, C. J.; Chen, T. H.; Jiang, J. Y.; Tseng, W. L., Lysozyme-directed synthesis of platinum nanoclusters as a mimic oxidase. *Nanoscale* **2014**, *6*, 9618-24.

- (9) Natalio, F.; Andre, R.; Hartog, A. F.; Stoll, B.; Jochum, K. P.; Wever, R.; Tremel, W., Vanadium pentoxide nanoparticles mimic vanadium haloperoxidases and thwart biofilm formation. *Nat. Nanotech.* **2012**, *7*, 530-5.

- (10) André, R.; Natálio, F.; Humanes, M.; Leppin, J.; Heinze, K.; Wever, R.; Schröder, H. C.; Müller, W. E. G.; Tremel, W., V₂O₅ Nanowires with an Intrinsic Peroxidase-Like Activity. *Adv. Funct. Mater.* **2011**, *21*, 501-509.

- (11) Asati, A.; Santra, S.; Kaitanis, C.; Nath, S.; Perez, J. M., Oxidase-like activity of polymer-coated cerium oxide nanoparticles. *Angew. Chem. Int. Ed.* **2009**, *48*, 2308-12.

- (12) Liang, H.; Lin, F.; Zhang, Z.; Liu, B.; Jiang, S.; Yuan, Q.; Liu, J., Multicopper Laccase Mimicking Nanozymes with Nucleotides as Ligands. *ACS Appl. Mater. Interfaces* **2017**, *9*, 1352-1360.

- (13) Feng, D.; Gu, Z. Y.; Li, J. R.; Jiang, H. L.; Wei, Z.; Zhou, H. C., Zirconium-metalloporphyrin PCN-222: mesoporous metal-organic frameworks with ultrahigh stability as biomimetic catalysts. *Angew. Chem. Int. Ed.* **2012**, *51*, 10307-10.

- (14) Wang, J.; Huang, R.; Qi, W.; Su, R.; Binks, B. P.; He, Z., Construction of a bioinspired laccase-mimicking nanozyme for the degradation and detection of phenolic pollutants. *Appl. Catal. B Environ.* **2019**, *254*, 452-462.

- (15) Cheng, H.; Zhang, L.; He, J.; Guo, W.; Zhou, Z.; Zhang, X.; Nie, S.; Wei, H., Integrated Nanozymes with Nanoscale Proximity for in Vivo Neurochemical Monitoring in Living Brains. *Anal. Chem.* **2016**, *88*, 5489-97.

- (16) Qin, L.; Wang, X.; Liu, Y.; Wei, H., 2D-Metal-Organic-Framework-Nanozyme Sensor Arrays for Probing Phosphates and Their Enzymatic Hydrolysis. *Anal. Chem.* **2018**, *90*, 9983-9989.

- (17) Wang, H.; Li, P.; Yu, D.; Zhang, Y.; Wang, Z.; Liu, C.; Qiu, H.; Liu, Z.; Ren, J.; Qu, X., Unraveling the Enzymatic Activity of Oxygenated Carbon Nanotubes and Their Application in the Treatment of Bacterial Infections. *Nano Lett.* **2018**, *18*, 3344-3351.

- (18) Fan, K.; Xi, J.; Fan, L.; Wang, P.; Zhu, C.; Tang, Y.; Xu, X.; Liang, M.; Jiang, B.; Yan, X.; Gao, L., In vivo guiding nitrogen-doped carbon nanozyme for tumor catalytic therapy. *Nat Commun* **2018**, *9*, 1440.

- (19) Luo, W.; Zhu, C.; Su, S.; Li, D.; He, Y.; Huang, Q.; Fan, C., Self-Catalyzed, Self-Limiting Growth of Glucose Oxidase-Mimicking Gold Nanoparticles. *ACS Nano* **2010**, *4*, 7451-7458.

- (20) Komkova, M. A.; Karyakina, E. E.; Karyakin, A. A., Catalytically Synthesized Prussian Blue Nanoparticles Defeating Natural Enzyme Peroxidase. *J. Am. Chem. Soc.* **2018**, *140*, 11302-11307.

- (21) Jiao, X.; Song, H.; Zhao, H.; Bai, W.; Zhang, L.; Lv, Y., Well-redispersed ceria nanoparticles: Promising peroxidase mimetics for H₂O₂ and glucose detection. *Anal. Methods* **2012**, *4*, 3261-3267.

- (22) Ge, C.; Fang, G.; Shen, X.; Chong, Y.; Wamer, W. G.; Gao, X.; Chai, Z.; Chen, C.; Yin, J. J., Facet Energy versus Enzyme-like Activities: The Unexpected Protection of Palladium Nanocrystals against Oxidative Damage. *ACS Nano* **2016**, *10*, 10436-10445.

- (23) Jalilov, A. S.; Nilewski, L. G.; Berka, V.; Zhang, C.; Yakovenko, A. A.; Wu, G.; Kent, T. A.; Tsai, A. L.; Tour, J. M., Perylene Diimide as a Precise Graphene-like Superoxide Dismutase Mimetic. *ACS Nano* **2017**, *11*, 2024-2032.

- (24) Mu, J.; Zhang, L.; Zhao, M.; Wang, Y., Catalase mimic property of Co₃O₄ nanomaterials with different morphology and its application as a calcium sensor. *ACS Appl. Mater. Interfaces* **2014**, *6*, 7090-8.

- (25) Chen, J.; Huang, L.; Wang, Q.; Wu, W.; Zhang, H.; Fang, Y.; Dong, S., Bio-inspired nanozyme: a hydratase mimic in a zeolitic imidazolate framework. *Nanoscale* **2019**, *11*, 5960-5966.

- (26) Jiang, D.; Ni, D.; Rosenkrans, Z. T.; Huang, P.; Yan, X.; Cai, W., Nanozyme: new horizons for responsive biomedical applications. *Chem. Soc. Rev.* **2019**, *48*, 3683-3704.

- (27) Sharma, T. K.; Ramanathan, R.; Weerathunge, P.; Mohammadtaheri, M.; Daima, H. K.; Shukla, R.; Bansal, V., Aptamer-mediated 'turn-off/turn-on' nanozyme activity of gold nanoparticles for kanamycin detection. *Chem. Commun.* **2014**, *50*, 15856-9.

1 (28) Tian, L.; Qi, J.; Oderinde, O.; Yao, C.; Song, W.; Wang, Y.,
2 Planar intercalated copper (II) complex molecule as small molecule
3 enzyme mimic combined with Fe₃O₄ nanozyme for bienzyme
4 synergistic catalysis applied to the microRNA biosensor. *Biosens.*
5 *Bioelectron.* **2018**, *110*, 110-117.

6 (29) Huang, Y.; Ran, X.; Lin, Y.; Ren, J.; Qu, X., Self-assembly of
7 an organic-inorganic hybrid nanoflower as an efficient biomimetic
8 catalyst for self-activated tandem reactions. *Chem. Commun.* **2015**,
9 *51*, 4386-9.

10 (30) Duan, D.; Fan, K.; Zhang, D.; Tan, S.; Liang, M.; Liu, Y.;
11 Zhang, J.; Zhang, P.; Liu, W.; Qiu, X.; Kobinger, G. P.; Gao, G. F.;
12 Yan, X., Nanozyme-strip for rapid local diagnosis of Ebola. *Biosens.*
13 *Bioelectron.* **2015**, *74*, 134-41.

14 (31) Chen, Z.; Wang, Z.; Ren, J.; Qu, X., Enzyme Mimicry for
15 Combating Bacteria and Biofilms. *Acc. Chem. Res.* **2018**, *51*, 789-
16 799.

17 (32) Gong, J.; Flaherty, D. W.; Yan, T.; Mullins, C. B., Selective
18 oxidation of propanol on Au(111): mechanistic insights into aerobic
19 oxidation of alcohols. *Chemphyschem* **2008**, *9*, 2461-6.

20 (33) Long, R.; Mao, K.; Ye, X.; Yan, W.; Huang, Y.; Wang, J.; Fu,
21 Y.; Wang, X.; Wu, X.; Xie, Y.; Xiong, Y., Surface facet of palladium
22 nanocrystals: a key parameter to the activation of molecular oxygen
23 for organic catalysis and cancer treatment. *J. Am. Chem. Soc.* **2013**,
24 *135*, 3200-7.

25 (34) Shen, X.; Liu, W.; Gao, X.; Lu, Z.; Wu, X.; Gao, X.,
26 Mechanisms of Oxidase and Superoxide Dismutation-like Activities
27 of Gold, Silver, Platinum, and Palladium, and Their Alloys: A
28 General Way to the Activation of Molecular Oxygen. *J. Am. Chem.*
29 *Soc.* **2015**, *137*, 15882-91.

30 (35) Liu, Y.; Wu, H.; Chong, Y.; Wamer, W. G.; Xia, Q.; Cai, L.;
31 Nie, Z.; Fu, P. P.; Yin, J. J., Platinum Nanoparticles: Efficient and
32 Stable Catechol Oxidase Mimetics. *ACS Appl. Mater. Interfaces*
33 **2015**, *7*, 19709-17.

34 (36) Liu, Y.; Zhou, M.; Cao, W.; Wang, X.; Wang, Q.; Li, S.; Wei,
35 H., Light-Responsive Metal-Organic Framework as an Oxidase
36 Mimic for Cellular Glutathione Detection. *Anal. Chem.* **2019**, *91*,
37 8170-8175.

38 (37) Selmeczi, K.; Réglér, M.; Giorgi, M.; Speier, G., Catechol
39 oxidase activity of dicopper complexes with N-donor ligands. *Coord.*
40 *Chem. Rev.* **2003**, *245*, 191-201.

41 (38) Ünal, M. Ü., Properties of polyphenol oxidase from Anamur
42 banana (*Musa cavendishii*). *Food Chem.* **2007**, *100*, 909-913.

43 (39) Klabunde, T.; Eicken, C.; Sacchettini, J. C.; Krebs, B., Crystal
44 structure of a plant catechol oxidase containing a dicopper center.
45 *Nature* **1998**, *5*, 1084-1090.

46 (40) Liu, Q.; Song, Y.; Ma, Y.; Zhou, Y.; Cong, H.; Wang, C.; Wu,
47 J.; Hu, G.; O'Keeffe, M.; Deng, H., Mesoporous Cages in Chemically
48 Robust MOFs Created by a Large Number of Vertices with Reduced
49 Connectivity. *J. Am. Chem. Soc.* **2019**, *141*, 488-496.

50 (41) Barrios-Estrada, C.; de Jesus Rostro-Alanis, M.; Munoz-
51 Gutierrez, B. D.; Iqbal, H. M. N.; Kannan, S.; Parra-Saldivar, R.,
52 Emergent contaminants: Endocrine disruptors and their laccase-
53 assisted degradation - A review. *Sci. Total Environ.* **2018**, *612*, 1516-
54 1531.

55 (42) Hou, M. F.; Tang, X. Y.; Zhang, W. D.; Liao, L.; Wan, H. F.,
56 Degradation of pentachlorophenol by potato polyphenol oxidase. *J.*
57 *Agric. Food. Chem.* **2011**, *59*, 11456-60.

